J Mater Sci (2013) 48:7994–8002
DOI 10.1007/s10853-013-7611-3

Sol–gel derived Ag-doped ZnO thin film for UV photodetector with enhanced response

Akshta Rajan · Harish Kumar Yadav · Vinay Gupta · Monika Tomar

Received: 25 April 2013 / Accepted: 18 July 2013 / Published online: 1 August 2013

Abstract Ultraviolet (UV) photodetectors based on pure zinc oxide (ZnO) and Ag-doped ZnO (Ag:ZnO) thin films with different Ag doping contents (0.05, 0.15, 0.65, 1.30 and 2.20 %) have been prepared by sol–gel technique. Photoresponse characteristics of the prepared detectors have been studied for UV radiation of $\lambda = 365$ nm and intensity = 24 μW/cm^2. The Ag:ZnO thin film-based photodetector having an optimum amount of 0.15 at. wt% Ag dopant exhibits a high photoconductive gain ($K = 1.32 \times 10^3$) with relatively fast recovery ($T_{37\ \%} = 600$ ms) and minimal persistence in comparison to other prepared photodetectors. The incorporation of Ag dopant (≤0.15 %) at Zn lattice sites (Ag_{zn}) in ZnO creates acceptor levels in the forbidden gap, thereby reducing the value of dark current. Upon illumination with UV radiation, the photogenerated holes recombine with the captured electrons at the Ag_{zn} sites. The photogenerated electrons increase the concentration of conduction electrons, thereby giving an enhanced photoresponse for Ag:ZnO photodetector (0.15 % Ag). At higher dopant concentration (≥0.65 %), Ag incorporated at the interstitial sites of ZnO leads to the formation of deep energy levels below the conduction band along with increase in oxygen-related defects, thereby giving higher values of dark current. The incorporation of Ag at interstitial sites results in degradation of photoresponse along with the appearance of persistence in recovery of the photodetector in the absence of UV radiation.

A. Rajan · V. Gupta
Department of Physics and Astrophysics, University of Delhi, Delhi 110007, India

H. K. Yadav
Physics Department, St.Stephen's College, University of Delhi, Delhi 110007, India

M. Tomar (✉)
Physics Department, Miranda House, University of Delhi, Delhi 110007, India
e-mail: monikatomar@gmail.com

Introduction

The detection of ultraviolet (UV) radiations is of prime importance in many commercial, military and scientific areas, such as ozone layer monitoring, flame detection, missile warning systems, medicine, accurate measurement of radiation for the treatment of UV irradiated skin, UV astronomy etc. [1]. In the last few years, UV photodetectors based on wide band gap semiconductors such as GaN and ZnO have been reported [2, 3]. GaN has made a remarkable progress in the field of UV photodetectors, however, it demands expensive thin film growth process on epitaxially matched substrates [4]. Alternatively, ZnO possessing wurtzite crystallographic structure with a wide band gap (~3.3 eV) and optical properties similar to that of GaN has emerged as a potential candidate for short wavelength optoelectronic devices including light-emitting diodes, laser diodes and photodetectors [4–7]. ZnO, besides being radiation hard material with large exciton binding energy (~60 MeV), is advantageous for various applications [8]. Furthermore, textured ZnO thin films can be easily deposited on low-cost substrates like glass or fused quartz using various physical or chemical deposition techniques [9]. Due to excellent oxygen physisorption and photodesorption behaviour on their surface or grain boundaries, ZnO thin films have been successfully exploited for UV detector applications [6, 10]. However, the moderate response and poor response time are the major concerns for ZnO-based UV detectors [11].

The presence of defects on the surface or grain boundaries of ZnO thin films is known to play a crucial role in altering the electrical conduction property which in turn influences the photoresponse characteristics [12]. Several efforts are being made globally to tailor the defect profile in ZnO either by doping with appropriate metal or altering the growth kinetics for desired photodetector application [13]. It is reported that incorporation of various metals in ZnO in different forms including dopants, overlayer and nanoparticles is useful in improving the photoconducting properties of ZnO [6, 14]. ZnO when doped with appropriate foreign element, results in the formation of acceptor or donor levels in the forbidden band gap, thereby altering its optical and electrical properties for practical detector applications. The doping of Ag in ZnO is reported either at the substitutional Zn sites or at the interstitial sites [15]. Therefore, incorporation of Ag dopant in ZnO lattice shows an amphoteric behaviour. Ag dopant in ZnO may form a deep level of about 0.23 eV below the conduction band, and an acceptor level of about 0.2 eV above the valence band in the forbidden gap [16, 17]. Several reports are available in the literature on the growth and characterization of Ag-doped ZnO thin films [18]. However, not much efforts have been made towards the fabrication of UV photodetector based on Ag-doped ZnO thin film despite of the fact that amphoteric behaviour of silver dopant in ZnO plays a major role in altering the electrical conductivity significantly [15].

In the present work, a highly sensitive UV photodetector has been realized using silver-doped ZnO (Ag:ZnO) thin film deposited by sol–gel technique. Concentration of silver dopant in ZnO film has been varied from 0.05 to 2.20 at. wt% and photoresponse parameters including dark current, photocurrent, photoconductive gain etc. have been studied.

Experimental

Pure and Ag-doped ZnO (Ag:ZnO) thin films with different dopant concentrations (0.05–2.20 %) were deposited using sol–gel technique. Zinc acetate dihydrate [$Zn(CH_3COO)_2 \cdot 2H_2O$] purchased from Sigma-Aldrich (≥99 % pure) was used as a starting material, whereas methanol and monoethanolamine (MEA) were used as a solvent and stabilizer respectively. The 0.23 M zinc acetate dihydrate was first dissolved in a mixture of methanol and silver nitrate ($AgNO_3$) (Fisher scientific, 99.8 % pure) and subsequently MEA was added in the molar ratio of 1.0 [19]. The prepared Zn complex solution was stirred for a time frame of 2–3 min. The concentration of Ag dopant was varied in atomic weight percentage from 0 to 2.20 by varying the Ag:Zn ratio. The UV photodetector has been fabricated by depositing ZnO and Ag:ZnO thin films on platinum (Pt) interdigital electrodes (IDEs) patterned corning glass substrates. Figure 1 shows the schematic of the structure of UV photodetector device with Ag:ZnO thin film as photoconductive material. For the patterning of IDEs, 80 nm thin layer of Pt was deposited on corning glass substrate by rf sputtering technique using a 3-in. diameter metallic Pt (99.99 % pure) target in 100 % Ar gas ambient and rf power of 100 W. To improve the adhesion of Pt layer on glass substrate, a buffer layer of titanium (10 nm) was sputtered prior to Pt deposition on the corning glass substrate in situ under similar deposition conditions. IDEs were patterned on glass substrates (IDE/glass) using the conventional photolithographic technique. The prepared Zn complex solution was spin coated over the IDE/glass substrates. After each coating, the film was dried in air at 300 °C for 3–5 min to evaporate the solvent and remove the organic residuals. The procedure from coating to drying was repeated until the desired thickness of the ZnO thin film was achieved. The optimization of the thickness of ZnO thin film with respect to UV photoresponse characteristics is reported elsewhere and was maintained at 221 nm for all deposited ZnO and Ag:ZnO thin films. The deposited thin films were annealed at 575 °C for 1 h in a temperature-controlled tubular furnace under atmospheric air to achieve desired crystallinity. In order to investigate the structural and optical properties of the grown thin films, ZnO and Ag:ZnO thin films of 221 nm thickness were deposited on bare corning glass substrate under identical growth conditions.

The crystallinity and surface morphology of thin films were analyzed by X-ray diffraction (XRD) (Bruker D8 Discover) and scanning electron microscope (SEM) respectively. The optical properties were studied using UV–Vis spectrophotometer (Perkin Elmer lambda 35) over the range 300–1100 nm. Thickness and surface roughness measurements of thin films were carried out using surface profiler (Veeco Dektak 150). The photoluminescence (PL) spectra were obtained at room temperature using PL spectroscopy (Horiba Jobin-Yvon LabRAM) with He–Cd

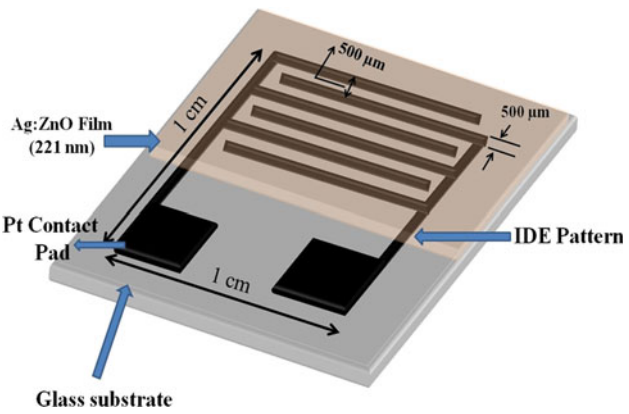

Fig. 1 Schematic of the UV photodetector

laser ($\lambda = 325$ nm) to study the defect profile of the pure and Ag-doped ZnO thin films.

Steady-state photoresponse of the UV photodetectors based on pure ZnO and Ag:ZnO thin films was measured at a fixed bias of 5 V under metal–semiconductor–metal (MSM) configuration by illuminating the samples using a UV lamp ($\lambda = 365$ nm, intensity = 24 μW/cm^2) as radiation source. Intensity of the UV light was measured with the help of an optical power meter (Newport, Model no 1830C). The transient photoresponse of prepared photodetectors was recorded at room temperature using semiconductor characterization system (Keithley 4200 SCS). The photoconductive gain of a UV photodetector is defined as $K = I_{on}/I_{off}$, where I_{on} is the photocurrent measured by illuminating the photodetector with UV radiations and I_{off} is the dark current measured without any illumination.

Results and discussion

Structural and optical properties

The ZnO and Ag:ZnO thin films were found to be smooth, transparent and strongly adherent to the corning glass substrates. Figure 2 shows the XRD patterns of pure and Ag-doped ZnO thin films having different doping concentrations of Ag in at. wt%. Pure ZnO thin film is labelled as Z0 and doped samples having 0.05, 0.15, 0.65, 1.30 and 2.20 % Ag are labelled as Z1, Z2, Z3, Z4 and Z5 respectively. It can be observed from the XRD pattern (Fig. 2) that all the deposited thin films (Z0–Z5) exhibit the peaks corresponding to hexagonal wurtzite structure of ZnO, indicating the growth of polycrystalline thin films. The dominant (002) peak along with weak diffraction peaks corresponding to (100) and (101) planes of ZnO (Fig. 2) were observed in the XRD pattern of all thin films showing deposition of preferred oriented thin films along (002) plane with *c*-axis normal to the substrate. No additional XRD peak was observed corresponding to any secondary phase related to Ag in Ag:ZnO thin films indicating the possible substitution of Ag ions at Zn sites in ZnO lattice. The results obtained from the XRD data for all the prepared thin films are summarized in Table 1. The 2θ value corresponding to (002) XRD peak was found to be 34.36° for pure ZnO thin film, which is slightly lower than the corresponding value (34.42°) reported for bulk ZnO. Position of all XRD peaks corresponding to ZnO is found to shift towards lower angles with the increasing concentration of Ag dopant in ZnO (Fig. 2). The observed shift in 2θ may be associated with the presence of stress in the prepared thin films [5]. It may be noted that Ag has relatively larger radii (1.22 Å) compared to that of Zn (0.6 Å) [20]. Therefore, unit cell of ZnO is expected to expand along the *c*-axis when Ag ions are substituted at Zn lattice sites, thereby inducing stress in the grown thin films. The peak position (2θ) corresponding to (002) reflection (Table 1) keeps on decreasing from 34.36° to 34.32° with the increase in Ag doping from 0.05 to 0.65 % in ZnO, and thereafter saturates at higher doping (>0.65 %). The values of lattice parameters of all prepared thin films using XRD data were estimated and are given in Table 1. The lattice constant, '*c*' of all the prepared thin films was found to be slightly higher in comparison to that of bulk ZnO (Table 1). The observed expansion in lattice parameter '*c*' for Ag:ZnO thin film (≤0.65 % Ag) may be related to the fact that the Ag dopant of larger ionic radii is being substituted at the Zn lattice sites. However, when the concentration of Ag dopant (>0.65 %) is further increased, Ag tends to occupy the interstitial sites, thereby giving a saturated value of lattice constant '*c*' (Table 1). The obtained results are in accordance with the results as reported earlier by Zheng et al. [21] and Blinks et al. [22] in which Ag was observed to be incorporated in ZnO at both the substitutional and interstitial sites. The value of crystallite size was evaluated using the well-known Scherrer's formula $d = K\lambda/\beta\cos\theta$, where K is 0.94, λ is X-ray wavelength (1.5406 Å), β is full width at half maxima (FWHM) of the dominant (002) XRD peak and θ is the corresponding diffraction angle. The estimated value of the crystallite size of ZnO thin film was about 27 nm. The crystallite size was found to be decreasing from 27 to 19 nm with the increase in the concentration of Ag dopant from 0 to 2.2 at. wt% in ZnO (Table 1).

Figure 3a–f shows the SEM microimages of the surface of all the prepared pure and Ag-doped ZnO thin films (Z0, Z1, Z2, Z3, Z4 and Z5). SEM images indicate that the prepared thin films exhibit a smooth surface morphology with uniformly distributed grains of nanosize (Fig. 3). The pure ZnO thin film (Z0) shows a dense and smooth surface morphology (Fig. 3a). An appreciable change in the surface microstructure has been observed with the doping of Ag in ZnO film. It is interesting to note from Fig. 3b–f that the agglomeration of crystallites takes place with the incorporation of Ag dopant in the ZnO thin film. Further, the porosity of thin films is also seen to be increasing with Ag doping in ZnO, and found to be maximum for the sample Z2 having 0.15 % Ag doping (Fig. 3c). When the concentration of Ag dopant is further increased (>0.15 %), a decrease in the porosity is observed and may be attributed to the incorporation of the excess Ag dopant at the interstitial sites in ZnO.

Figure 4 shows the UV–Vis transmittance spectra of the ZnO and Ag:ZnO thin films deposited on corning glass substrates. Undoped ZnO thin film is highly transparent (~80 %) in the visible region and onset of a sharp fundamental absorption edge at around 380 nm is observed

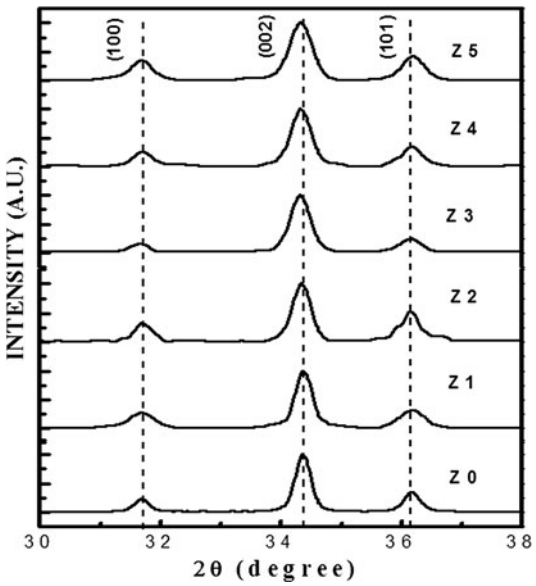

Fig. 2 XRD pattern of the pure ZnO (Z0) and Ag-doped ZnO thin films (Z1, Z2, Z3, Z4, Z5) having varying Ag doping % (Z1 = 0.03 %, Z2 = 0.13 %, Z3 = 0.65 %, Z4 = 1.31 % and Z5 = 2.19 % Ag by atomic weight percent)

(Fig. 4). The optical transmittance was improved with the doping of Ag in ZnO thin film up to 0.15 at. wt% and is attributed to the substitution of Ag at Zn lattice site (Fig. 4). However, the transmittance is found to decrease with the incorporation of excess Ag dopant (>0.13 %). The transmittance observed in Ag:ZnO (>0.13 %) is even less than that obtained for undoped ZnO sample and may be due to the loss of incident light from the scattering centres provided by the Ag ions at the interstitial site in doped ZnO. Optical band gap (E_g) of the Ag:ZnO thin films was evaluated by extrapolating the linear portion of Tauc plot between $(\alpha h\upsilon)^2$ versus $h\upsilon$ to $\alpha = 0$, where α is the absorption coefficient and $h\upsilon$ is the photon energy (inset of Fig. 4). Estimated value of the band gap was about 3.28 eV for the undoped ZnO thin film (Z0 sample) and is in good agreement with the corresponding values (3.20–3.28 eV) as reported by other workers for ZnO thin films grown using different techniques [5, 9, 23, 24]. The variation of the band gap of Ag:ZnO thin films as a function of the concentration of Ag dopant is shown in Fig. 5. The value of band gap was found to be decreasing continuously from 3.26–3.23 eV with the increase in concentration of Ag dopant in the Ag:ZnO thin film from 0.05 to 2.20 at. wt% (Fig. 5). It may be noted from Fig. 5 that reduction in the value of band gap of Ag:ZnO thin film is significant for lower concentration of Ag doping (≤0.65 %), and thereafter shows a saturating tendency. This may be related to the fact that at lower Ag doping concentration (≤0.15 %), Ag is substituted at Zn^{2+} sites resulting in a change in band structure [25]. On the other hand, at higher concentration of Ag dopant (>0.15 %), the presence of Ag at the interstitial sites in ZnO may be responsible for the observed saturating value of band gap (Fig. 5).

The room temperature PL spectra obtained for pure ZnO and Ag:ZnO thin films are shown in Fig. 6. Two emission peaks centred at around 3.3 and 2.4 eV were observed in all PL spectra (Fig. 6). The peak at around 3.3 eV is the characteristic emission peak for ZnO corresponding to the near band edge (NBE) emission and is expected to arise from the recombination of free exciton [26]. The other broad emission peak (∼2.4 eV) in the visible region (Fig. 6) corresponds to the deep level emission arising due to the presence of point defects in the Ag:ZnO thin films. The values of band gap estimated from the NBE peak are presented in Table 1, and are in good agreement with the corresponding values obtained from UV–Vis transmittance study. An appreciable red shift in the NBE peak position is observed with incorporation of Ag dopant in ZnO thin films. The NBE peak was found to shift continuously towards lower energy with the increase in Ag content (0–2.20 %) in ZnO film (Fig. 6). Also, it is interesting to note from Fig. 6 that the NBE peak gets broadened with increase in the Ag doping concentration, especially for Ag content >0.15 %. The doping of Ag in ZnO is known to create both acceptor/donor levels in the forbidden gap

Table 1 Various parameters calculated from XRD, UV–Vis and PL studies (1) 2θ, (2) crystallite size, (3) lattice constant 'c' and (4) band gap

Concentration of Ag (at. wt%)	Sample code	2θ (°)	Crystallite size (nm)	Lattice constant 'c' (Å)	Lattice constant 'a' (Å)	Band gap (eV)	
						UV–Vis	PL
0	Z0	34.36	27.5	5.216	3.256	3.28	3.30
0.05	Z1	34.35	24.4	5.217	3.258	3.26	3.27
0.15	Z2	34.34	22.7	5.219	3.256	3.25	3.26
0.65	Z3	34.32	21.5	5.222	3.258	3.24	3.25
1.30	Z4	34.32	21.3	5.222	3.256	3.24	3.25
2.20	Z5	34.32	18.6	5.222	3.258	3.23	3.24
Bulk	–	34.42	–	–	–	–	–

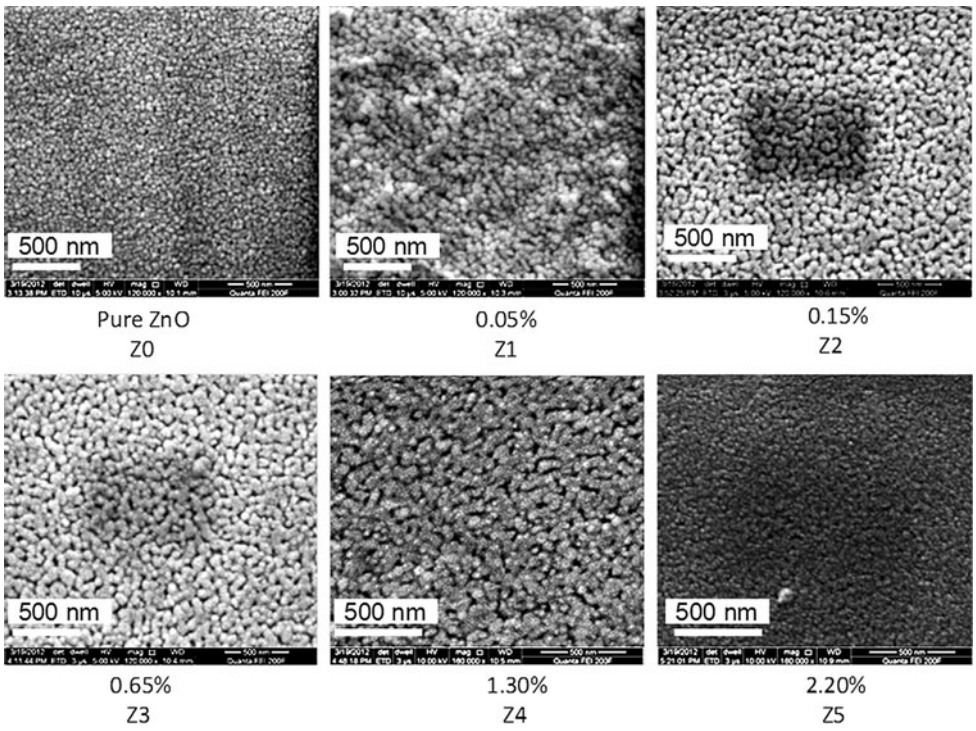

Fig. 3 SEM images of the pure ZnO (Z0) and Ag-doped ZnO thin films (Z1, Z2, Z3, Z4 and Z5)

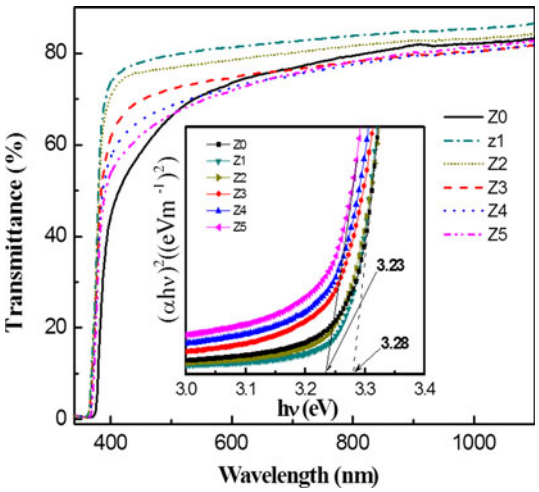

Fig. 4 UV–Vis spectra of the pure and Ag-doped ZnO thin films. Inset shows Tauc plot of the films

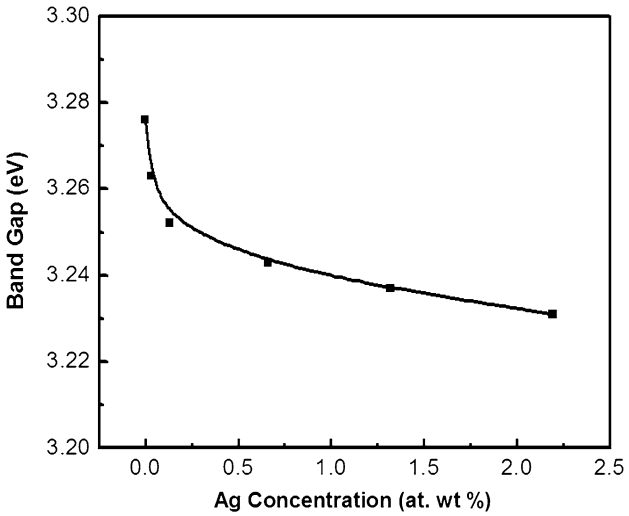

Fig. 5 Variation of band gap with Ag doping concentration in ZnO thin films

depending on the substitution of Ag at Zn lattice site or interstitial site, and thus leads to multiple allowed transitions [20]. The defect peak at about 2.4 eV is found to exhibit an interesting behaviour on introduction of Ag in ZnO. A broad and well-defined emission peak observed at around 2.5 eV in pure ZnO thin film (Fig. 6) indicates the presence of native point defects in the as-deposited film. The relative intensity of defect emission peak with respect to the NBE peak (I_{vis}/I_{UV}) changes significantly with Ag doping (Fig. 6). At lower doping concentration of Ag ($\leq$0.15 %), the intensity of the defect emission peak with respect to NBE peak (I_{vis}/I_{UV}) increases with Ag doping. The observed variation at lower concentration of Ag doping may be attributed to the incorporation of most of the dopant Ag^{+} ions at Zn^{2+} substitutional sites in ZnO lattice. It may be noted from Fig. 6 that the sample Z2 (0.15 % Ag dopant) exhibits minimum intensity of defect emission peak with respect to the NBE peak indicating that most of the Ag dopant ions are being substituted at the Zn lattice sites in Ag:ZnO film (sample Z2) having minimum concentration of native defects. To understand the effect of Ag dopant on the defect profile of ZnO thin film, the emission

peaks in PL spectra were deconvoluted. Both NBE and defect emission peaks were deconvoluted into two and four subpeaks respectively, and are shown in Fig. 6 for all the prepared thin film samples. The incorporation of Ag in ZnO is reported to exhibit the emission peak corresponding to 3.11 eV near NBE peak of ZnO [25]. Therefore, NBE peak was deconvoluted into two subpeaks, one centred at around 3.11 eV and another corresponding to the respective band gap values of the Ag:ZnO thin film samples. However, defect emission peak was deconvoluted into four subpeaks centred at 2.90, 2.50, 2.35 and 2.64 eV corresponding to the electronic transitions related to various defects including Zn interstitial, oxygen vacancies, oxygen antisites and zinc interstitial to zinc vacancies (Z_i–Z_v) respectively [27]. The intensity of deconvoluted subpeaks obtained for all prepared Ag:ZnO thin films are summarized in Table 2a and b. It may be noted from Table 2a that an additional emission peak corresponding to 3.11 eV was observed along with NBE peak for all thin film samples (Z1–Z5) prepared after incorporating Ag dopant. The intensity of 3.11 eV peak was found to be small in comparison to that of NBE peak for Ag:ZnO thin film having lower concentration (≤0.15 %) of Ag dopant (Fig. 6). However, the intensity of 3.11 eV peak increases significantly at higher concentration (≥0.65 %) of Ag dopant (Fig. 6). The observed results suggest that the Ag^{+} is substituting Zn^{2+} site in ZnO lattice for lower concentration (≤0.15 %) of Ag dopant, and are incorporating at interstitial positions for higher Ag dopant concentration. The deconvoluted subpeaks of defect emission (Table 2b) show that the native defects in the prepared Ag:ZnO thin films are minimum for sample (Z2) having 0.15 % Ag dopant concentration. However, the defects related to oxygen were found to increase significantly in the samples (Z3–Z5) prepared with higher concentration (≥0.65 %) of Ag dopant (Table 2b).

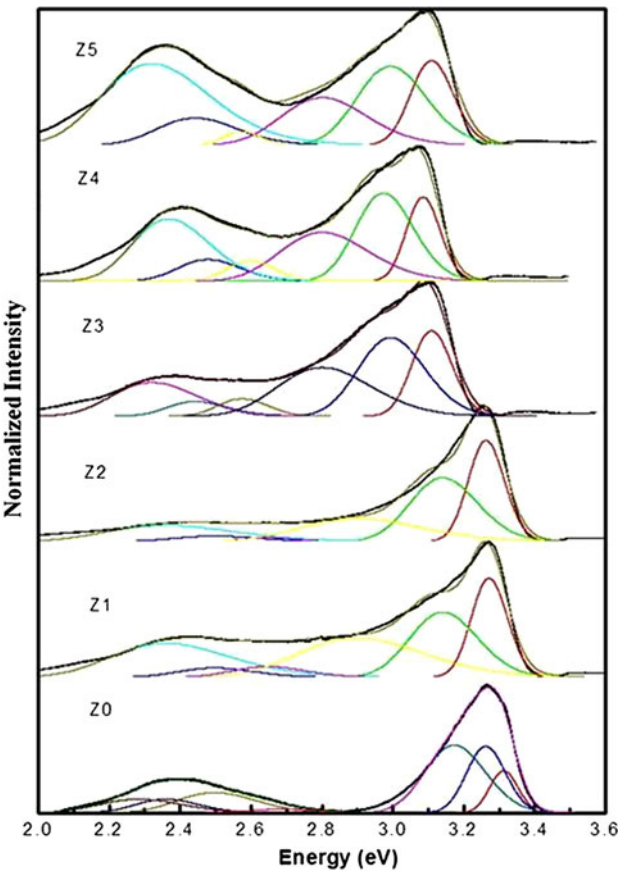

Fig. 6 Room temperature photoluminescence spectra of the pure and Ag:ZnO thin films

Sensing response characteristics

UV photoresponse characteristics of the pure and Ag-doped ZnO thin film photodetectors (Z0, Z1, Z2, Z3, Z4 and Z5) were investigated towards UV radiation of $\lambda = 365$ nm and intensity = 24 μW/cm^2 at a bias voltage of 5 V. The typical *I–V* characteristic of Ag:ZnO thin film structure having 0.15 % Ag doping concentration (sample Z2) was measured under dark and photoillumination condition and the obtained variation is shown in Fig. 7. A linear variation in the log–log plot of *I–V* curve obtained under both dark and photoillumination condition was observed (inset of Fig. 7) indicating an ohmic behaviour of the prepared metal electrode (Pt) with the oxide thin film (Ag:ZnO). The value of dark current was about 0.20 μA for sample Z2 at an applied bias of 5 V. The photocurrent measured under illumination of UV radiation (intensity = 24 μW/cm^2) was found to increase by about three orders of magnitude over the entire measured range of applied bias (Fig. 7) in comparison to the corresponding value of dark current (0.26 mA) at an applied bias of 5 V for sample Z2.

Figure 8 represents the time-dependent photoresponse transient characteristics of all the prepared ZnO and Ag:ZnO thin film-based UV photodetectors in the presence and absence of UV illumination. The photoresponse behaviour (Fig. 8) is similar to that normally observed in photoconducting ZnO samples by various workers [10]. It may be seen from Fig. 8 that when the UV illumination is off, all the prepared UV-photodetectors exhibit a low value of dark current I_{off} (∼μA). The current of all photodetectors was found to increase rapidly with time upon exposure to UV, and thereafter saturates at a particular level (Fig. 8) giving I_{on} (photocurrent). When the UV radiation is turned off (recovery period), current decreases slowly to attain its initial value (I_{off}). The presence of some persistence during recovery period especially for Ag:ZnO thin film photodetectors (Z3, Z4 and Z5) having higher concentration

Table 2 The value of intensities of deconvoluted emission peaks (a) two subpeaks of near band edge emission peak, (b) four subpeaks of defect emission

(a)

Sample prepared	Energy (eV)	Value of intensity	Energy (eV)	Value of intensity
Pure	3.31	0.57	–	–
0.05 %	3.27	0.73	3.13	0.48
0.15 %	3.26	0.74	3.13	0.48
0.65 %	3.24	0.63	3.11	0.58
1.30 %	3.25	0.62	3.11	0.65
2.20 %	3.24	0.62	3.11	0.58

(b)

Samples prepared	Zn_i (2.90 eV)	O_v (2.5 eV)	O_{anti} (2.35 eV)	Z_i–Z_v (2.64 eV)	I_{vis}/I_{UV}
Pure	–	0.18	0.14	0.08	–
0.05 %	0.29	0.07	0.25	0.08	1.521
0.15 %	0.17	0.04	0.12	0.03	1.575
0.65 %	0.36	0.11	0.25	0.13	1.090
1.30 %	0.36	0.16	0.46	0.15	0.960
2.20 %	0.35	0.20	0.60	0.10	1.070

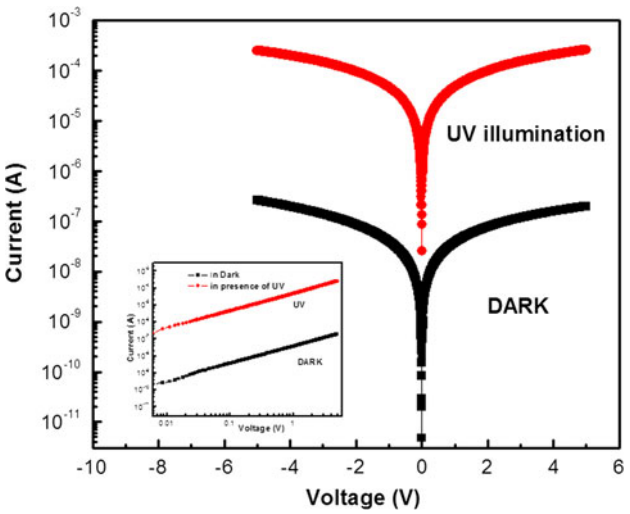

Fig. 7 *I–V* characteristics of the 0.13 % Ag-doped ZnO thin film sample (Z2)

(>0.15 % of Ag dopant) (Fig. 8) was observed and may be related to the presence of oxygen-related defects in the fabricated Ag:ZnO thin films. The variation in dark current and photocurrent obtained for photodetector samples are shown in Fig. 9 as a function of Ag dopant concentration. The values of dark current and photocurrent upon UV illumination (24 μW/cm^2 intensity) for pure ZnO thin film UV photodetector (sample Z0) at an applied bias of 5 V are found to be about 0.73 μA and 0.11 mA respectively. When Ag is incorporated into ZnO thin film, a continuous decrease in the value of dark current is observed from 0.73 to 0.11 μA with increase in concentration of Ag doping from 0 to 0.65 % (Fig. 9). However, the value of dark current increases significantly (Fig. 9) at higher concentration (>0.65 %) of Ag doping in ZnO thin film (Z4 and Z5). Similar trend in the behaviour of photocurrent with Ag dopant concentration was observed (Fig. 9). The photocurrent of prepared UV detectors decreases from 0.41 mA to 0.06 mA with increase in Ag doping concentration in ZnO from 0.05 to 0.65 % and increases to 0.62 mA with further increase in Ag dopant concentration to 2.20 %.

The photoconductive gain (K) of a detector is defined as

$$K = I_{on}/I_{off} \quad (1)$$

where I_{on} and I_{off} are the values of photocurrent and dark current of the photodetector respectively, measured under the presence and absence of UV illumination. Figure 10 shows the variation of photoconductive gain (K) of the prepared Ag:ZnO thin film-based UV photodetector as a function of Ag doping concentration. The photoconductive gain of pure ZnO thin film UV detector (Z0 sample) was about 1.5×10^2. The photoconductive gain of all photodetectors having Ag-doped ZnO thin films is much higher (Fig. 10) in comparison to that obtained for pure ZnO thin film-based UV detector except for sample Z5. It may be clearly seen from Fig. 10 that the photoconductive gain (K) is increasing from 1.5×10^2 to 1.3×10^3 with increase in Ag doping concentration in ZnO thin film from 0 to 0.15 % having a maximum value for Z2 (0.15 % Ag doping). However, on further increasing the Ag doping concentration (from 0.65 to 2.20 %), the photoconductive gain starts decreasing from 1.3×10^3 to 1.4×10^2 (Fig. 10). Therefore, UV photodetector based on Ag:ZnO

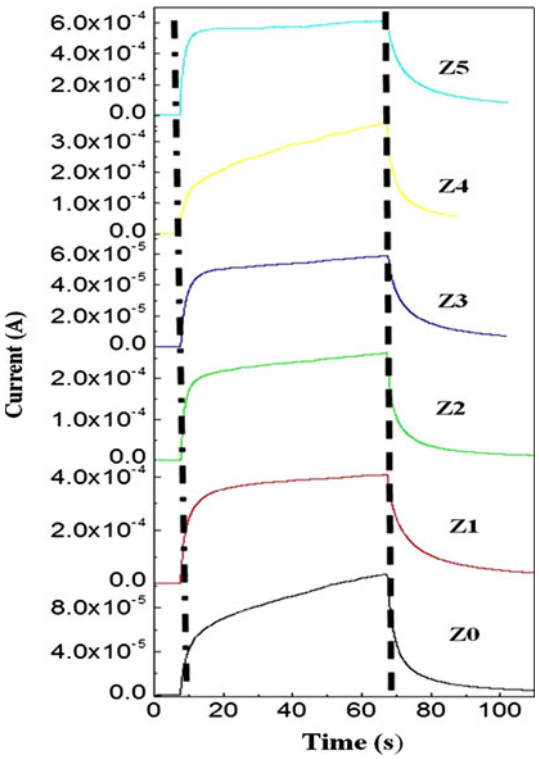

Fig. 8 Time-dependent on/off photoconduction measurements on the pure and Ag-doped ZnO thin film based UV photodetector in the presence of 24μW/cm^2

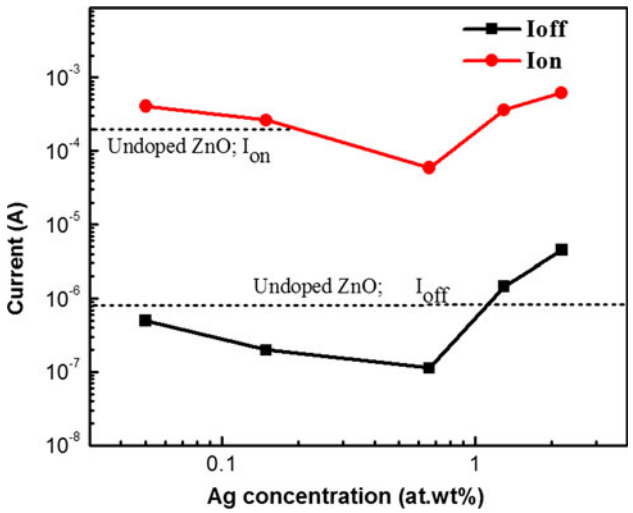

Fig. 9 Effect of silver doping on dark current and Photocurrent

thin film having 0.15 % Ag doping is found to exhibit enhanced response characteristics in comparison to other prepared photodetectors. The value of response time for all the prepared photodetectors has also been obtained and is shown in the inset of Fig. 10 as a function of the concentration of Ag dopant. The response time was found to decrease significantly with incorporation of Ag in ZnO for low dopant concentration (≤0.15 %) and becomes much higher at higher Ag dopant concentration (1.30 %).

A possible mechanism for the observed photoresponse characteristics of Ag:ZnO thin film photodetector is discussed in the following section. At lower Ag doping concentrations (≤0.15 %), Ag^+ is expected to occupy the Zn^{2+} sites in host ZnO lattice, as discussed earlier. The substitution of Ag^+ in ZnO lattice (Ag_{zn}) results in the formation of acceptor energy level in the forbidden gap about 0.2 eV above the valance band [25]. The free electrons available in the conduction band of Ag:ZnO may get trapped at Ag_{zn} site or recombine with the holes available in the valance band resulting in a decrease in carrier concentration. Therefore, the value of dark current of photodetector decreases with increase in concentration of Ag^+ at Zn^{2+} lattice site as observed in the present study (Fig. 9). At higher Ag dopant concentration, excess Ag^+ ions may tend to occupy interstitial sites in ZnO and lead to creation of large amount of structural defects [20]. The interstitial Ag may form a deep energy level in the forbidden gap at about 0.23 eV below the conduction band of ZnO [16]. Also, the intrinsic defects corresponding to interstitial Zn (Zn_i) and oxygen vacancies (O_v) increase with increase in Ag dopant concentration (Table 2b). Therefore, at higher Ag dopant concentration, dark current of photodetectors increases with increase in Ag concentration in Ag:ZnO thin film (Fig. 9).

The current (I_{on}) under the illumination of UV radiation increases significantly (in comparison to I_{off}) for all prepared pure ZnO and Ag:ZnO thin film photodetectors. The increase in photocurrent of pure ZnO thin film is attributed to the presence of oxygen defects on the surface or grain boundaries. These oxygen defects act as trap centres for the free electrons and become O_2^- after capturing conduction electrons. Under UV illumination, electron–hole pairs are

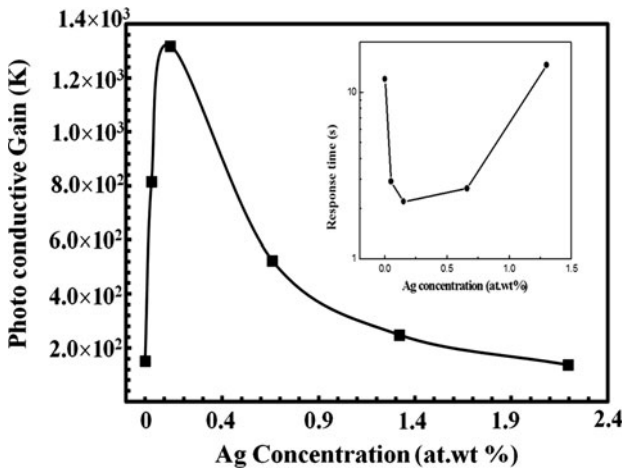

Fig. 10 Ag concentration dependence of the photoconductive gain. Inset showing variation of response time with concentration of Ag

generated in the ZnO thin film. The photogenerated holes recombine with the trapped electrons at oxygen defect sites and the photogenerated electrons increases the concentration of charge carriers in the conduction band, thereby giving a higher value of photocurrent (Fig. 9). The substitution of Ag^{+} at Zn^{2+} lattice site in ZnO results in the formation of trap centres for free electrons. The capturing of free electrons under dark conditions (without UV illumination) gives lower value of dark current for Ag:ZnO thin film. However, these trapped electrons are released under illumination of UV radiation, thereby increasing the photoconduction for Ag:ZnO thin film-based photodetectors in comparison to that obtained for pure ZnO thin film detector. The presence of Ag at interstitial sites for higher Ag doping concentrations ($\geq$0.65 %) reduces the concentration of photoelectrons in the conduction band of ZnO, and results in a small decrease in the photocurrent (Figs. 8, 9). It is imported to note from the PL studies that the oxygen-related defects become large with Ag doping at higher dopant concentration ($\geq$0.65 %). The presence of oxygen-related defects results in formation of multitrap energy levels in the forbidden gap of Ag:ZnO thin films which contribute to the multi transitions between conduction band and trap levels under UV illumination. Therefore, the persistence in the photoresponse was found to increase for Ag:ZnO thin films (samples Z3, Z4 and Z5) having higher Ag dopant concentration ($\geq$0.65 %) due to presence of multilevel trap levels. However, these defects were minimal in the sample Z2, giving an enhanced response with fast response time and without any persistence during the recovery.

Conclusion

c-Axis oriented ZnO and Ag:ZnO thin films have been deposited by sol–gel technique and utilized successfully for fabrication of UV photodetector in MSM configuration. The photoconductive gain for UV photodetector based on Ag:ZnO thin film having 0.15 % Ag content is about an order higher (1.32×10^{3}) compared to the corresponding value obtained for pure ZnO thin film photodetector (1.52×10^{2}). Substitution of Ag^{+} ions at the Zn^{2+} sites in ZnO lattice is responsible for obtaining an enhanced photoresponse along with low dark current. The photoresponse characteristics of UV photodetector degrades at higher Ag dopant concentration ($\geq$0.65 %) due to incorporation of Ag at the interstitial sites in ZnO resulting in higher value of dark current. The Ag:ZnO thin film having 0.15 at. wt% Ag content prepared by sol–gel technique exhibits enhanced photoresponse and less persistent behaviour under UV radiation of $\lambda = 365$ nm and intensity $= 24$ $\mu W/cm^2$. The presence of oxygen-related defects results in persistence in the recovery of these photodetectors. The obtained results in the present study are encouraging for the realization of an efficient UV photodetector.

Acknowledgements The authors acknowledge the financial support provided by the Department of Science and Technology (DST), Government of India for granting research sponsored project. One of the authors (A.R.) is thankful to UGC for research fellowship.

References

1. Xu ZQ, Deng H, Xie J, Li Y, Xu XT (2006) Appl Surf Sci 253:476
2. Zhao M, Bao J, Fan X, Gu F, Guo Y, Zhang Y, Zhao M, Sha Y, Guo F, Li J (2009) Phys B 404:275
3. Moon TH, Jeong MC, Lee W, Myoung JM (2005) Appl Surf Sci 240:280
4. Lee YC, Hassan Z, Yam FK, Abdulla MJ, Ibrahim K, Barmawi M, Sugianto, Budiman M, Arifin P (2005) Appl Surf Sci 249:91
5. Gupta V, Mansingh A (1996) J Appl Phys 80:1063
6. Yadav HK, Sreenivas K, Gupta V (2010) J Appl Phys 107:044507
7. Baltakesmez A, Tekmen S, Tuzemen S (2011) J Appl Phys 110:054502
8. Chen KJ, Hung FY, Chang SJ, Younga SJ (2009) J Alloys Compd 479:674
9. Mehan N, Gupta V, Sreenivas K, Mansingh A (2004) J Appl Phys 96:3134
10. Basak D, Amin G, Mallik B, Paul GK, Sen SK (2003) J Cryst Growth 256:73
11. Mridha S, Basak D (2006) Chem Phys Lett 427:62
12. Ghosh T, Basak D (2011) Mater Res Bull 46:1975
13. Kouklin N (2008) Adv Mater 20:2190
14. Mandalapu LJ, Xiu FX, Yang Z, Liu JL (2007) Solid-State Electron 51:1014
15. Fan J, Freer R (1995) J Appl Phys 77:4795
16. Kanai Y (1991) Jpn J Appl Phys 30:2021
17. Gruzintsev N, Volkov VT, Khodos II, Nikiforova TV, Koval'-chuk MN (2002) Russ Microelectron 31:200
18. Li Y, Zhao X, Fan W (2011) J Phys Chem C 115:3552
19. Sagar P, Shishodia PK, Mehra RM (2007) Appl Surf Sci 253:5419
20. Zeferino RS, Flores MB, Pal U (2011) J App Phys 109:014308
21. Zheng YH, Chen CQ, Zhan YY, Lin XY, Zheng Q, Wei KM, Zhu JF (2008) J Phys Chem C 112:10773
22. Blinks DJ, Grimes RW (1993) J Am Ceram Soc 76:2370
23. Li Y, Yao B, Lu YM, Cong CX, Zhang ZZ, Gai YQ, Zheng CJ, Li BH, Wei ZP, Shen DZ, Fan XW, Xiao L, Xu SC, Liu Y (2007) Appl Phys Lett 91:021915
24. Saha S, Mehan N, Sreenivas K, Gupta V (2009) Appl Phys Lett 95:071106
25. Liu K, Yang B, Yan H, Fu Z, Wen M, Chen Y, Zuo J (2009) J Lumin 129:969
26. Yadav HK, Shreenivas K, Katiyar RS, Gupta V (2007) J Phys D 40:6005
27. Wei X, Man B, Xue C, Chen C, Liu M (2006) Jpn J Appl Phys 45:8586